



## RESEARCH LETTER

10.1029/2018GL079767

### Key Points:

- We employ a three-dimensional climate model to simulate a warm Late Noachian Mars climate with mean annual temperature  $\sim 275$  K
- In this climate scenario, precipitation is dominated by snowfall, not rainfall
- Most water resides as ice in the highlands, not as an ocean in the lowlands; pluvial crater degradation and clay formation are unlikely

### Correspondence to:

A. M. Palumbo,  
ashley\_palumbo@brown.edu

### Citation:

Palumbo, A. M., & Head, J. W. (2018). Early Mars climate history: Characterizing a “warm and wet” Martian climate with a 3-D global climate model and testing geological predictions. *Geophysical Research Letters*, 45, 10,249–10,258. <https://doi.org/10.1029/2018GL079767>

Received 25 JUL 2018

Accepted 26 SEP 2018

Accepted article online 1 OCT 2018

Published online 13 OCT 2018

# Early Mars Climate History: Characterizing a “Warm and Wet” Martian Climate With a 3-D Global Climate Model and Testing Geological Predictions

Ashley M. Palumbo<sup>1</sup> and James W. Head<sup>1</sup>

<sup>1</sup>Department of Earth, Environmental and Planetary Sciences, Brown University, Providence, RI, USA

**Abstract** Observations of Late Noachian-Early Hesperian-aged Martian surfaces reveal valley networks, lakes, degraded craters, and putative oceanic shorelines, often interpreted to require a persistent “warm and wet” climate, characterized by mean annual temperature  $>273$  K and abundant rainfall. We simulate this “warm and wet” climate (global mean annual temperature  $\sim 275$  K) with a 3-D global climate model to determine whether these features could have formed in this climate through rainfall activity. We find that rainfall is limited in abundance and areal distribution, precipitation is dominated by snowfall, and highlands temperatures are  $<273$  K for the majority of the year. We conclude that, in this simulated climate scenario, (1) Late Noachian-Early Hesperian valley networks and lakes could not have formed through rainfall-related erosion, (2) crater degradation by rainsplash and runoff is not predicted, (3) global clay formation through long-lived rainfall, fluvial activity, and warm temperatures is unlikely, and (4) the presence of a rainfall- and overland flow-fed northern ocean is improbable.

**Plain Language Summary** Observations and analyses of Martian surface features, including fluvial and lacustrine features, imply that liquid water was abundant  $\sim 3.7$  Ga. The characteristics of these features has led researchers to conclude that the early climate was likely to have been “warm and wet”, characterized by abundant rainfall and surface runoff. Here we implement a three-dimensional climate model and simulate the conditions of a “warm and wet” climate scenario, with globally averaged surface temperature  $\sim 275$  K, just above the melting point of water, to determine whether these surface features could have actually formed in this climate scenario through rainfall-related activity. Contrary to previous predictions, we find that rainfall is extremely limited in this climate scenario, precipitation is dominated by snowfall, and temperatures are below freezing for the majority of the year in regions where the fluvial and lacustrine features are abundant. We suggest that snow accumulation, melting, and surface runoff may offer a more plausible explanation for the formation of these features.

## 1. Introduction

The Martian surface contains abundant geological evidence that liquid water was stable at the surface during the Late Noachian-Early Hesperian (LN-EH,  $\sim 3.7$  Ga), including widespread valley networks (VNs; Fassett & Head, 2008a; Hynes et al., 2010), open- and closed-basin lakes (Cabrol & Grin, 1999; Fassett & Head, 2008b; Goudge et al., 2015), and exposed aqueous alteration products (Bibring et al., 2006; Carter et al., 2015). These features are commonly cited as evidence that the LN-EH was much warmer and wetter than the current hyper-arid and hypothermal Amazonian climate, characterized by mean annual temperature (MAT)  $\geq 273$  K and rainfall and associated runoff as the dominant erosive mechanism (Craddock & Howard, 2002; Ramirez, 2017; Ramirez & Craddock, 2018). Additional evidence for a “warm and wet” climate includes the preservation state of Noachian-aged craters, which have degraded rims and no visible ejecta deposits (e.g., Jones, 1974), characteristics which have been attributed to rainsplash-related erosion (Craddock & Howard, 2002). The proposition of a “warm and wet” LN-EH climate has further led researchers to conjecture about the possibility of a Noachian ocean in the northern lowlands (Clifford, 1993; Parker et al., 1993), which is considered to be important for driving the vigorous hydrological cycle that would have been required for recycling of water and formation of VNs (Luo et al., 2017).

On the basis of these types of considerations, Craddock and Howard (2002) outlined the evidence for a “warm, wet early climate capable of supporting rainfall and surface runoff” and described this climate as “the most plausible scenario for explaining the entire suite of features in the Martian cratered highlands.”

Included in their suite of features were (1) degraded craters, whose morphology indicated that “modification occurred by creep induced by rainsplash combined with surface runoff and erosion”, and (2) VNs, whose morphology and drainage density are “entirely consistent with [formation through] rainfall and surface runoff.”

More recently, Ramirez and Craddock (2018) outlined the geological and climatological case for a warmer and wetter early Mars. They point out that “ancient terrains preserve landscapes consistent with stream channels, lake basins and possibly even oceans, and thus the presence of liquid water flowing on the Martian surface 4 Ga.” They argue that “a warm and semi-arid climate capable of producing rain is most consistent with the geological and climatological evidence” and that “the geomorphology cannot be explained without the occurrence of above-freezing surface temperatures and rain at least seasonally, if not persistently.”

Despite the widespread evidence for abundant liquid water activity at the surface, recent studies using advanced 3-D climate models have been unsuccessful in reproducing the continuous and long-lived “warm and wet” climate conditions interpreted to be necessary for the formation of the fluvial and lacustrine features and observed crater degradation when considering the influence of the faint young Sun (Gough, 1981) and reasonable greenhouse gas concentrations (e.g., Forget et al., 2013; Halevy & Head, 2014; Johnson et al., 2008; Mischna et al., 2013; Postawko & Kuhn, 1986; Wordsworth et al., 2013). Instead, the models predict a “cold and icy” climate, characterized by global MAT  $\sim 225$  K, far below the melting point of water (Forget et al., 2013; Wordsworth et al., 2013). Under atmospheric pressure conditions higher than a few tens of millibar, the atmosphere and surface thermally couple, inducing an adiabatic cooling effect (Wordsworth et al., 2013); the resulting dominant altitude dependence of temperature causes water to be distributed as ice in the highlands (Head & Marchant, 2014; Wordsworth et al., 2013).

But what would a Late Noachian Mars with a “warm and wet/arid” climate be like? Previous work by Wordsworth et al. (2015) used a 3-D global climate model (GCM) to compare the predicted “cold and icy” climate with the long sought-after “warm and wet” climate; Wordsworth et al. (2015) forced the “warm and wet” climate in the model by implementing either an unrealistically high solar flux or intense artificial greenhouse warming and by altering topography and albedo to imitate the presence of a lowlands ocean. Specifically, for their “warm and wet” simulations, they were interested in simulating a climate with continuous warm conditions, characterized by global MAT  $\sim 283$  K, similar to the present global MAT on Earth, a long-lived and ice-free ocean in the lowlands with a shoreline at  $-2.54$  km (following Achille & Hynes, 2010), and a vigorous rainfall-dominated hydrological cycle. Wordsworth et al. (2015) found that the distribution of rainfall in this climate scenario is not well correlated with the VN density distribution. However, this climate scenario and the nature of the associated hydrological cycle are likely to be a function of the global temperatures and the forced presence of a large, stable ocean.

Thus, in order to test the observations, predictions, and interpretations of Craddock and Howard (2002) and Ramirez and Craddock (2018), we have modeled a warm LN-EH climate with “above freezing surface temperatures” (global MAT, of  $\sim 275$  K, 2 K above the melting point of water); the climate we model here is colder than that considered by Wordsworth et al. (2015), representing the coldest possible “warm and wet” climate, and the simulations are not initiated with an ocean forced in the lowlands. Wordsworth et al. (2015) had to mimic the characteristics of an ocean because the model did not naturally predict a long-lived, stable ocean; we do not repeat this analysis because we are interested in model-predicted locations of surface ponding and choose not to force the lowlands as a water sink or source. We perform our analysis in order to document the nature of a “warm and wet” climate, to assess the type of precipitation that is predicted to occur, and to assess how its location and amount compare to the distribution of VNs, lakes, degraded craters, and a putative northern ocean. We specifically test the predictions and points outlined in Craddock and Howard (2002) and Ramirez and Craddock (2018) that (1) rainfall occurs “at least seasonally, if not persistently”; (2) rainfall patterns and locations are coincident with the occurrence and density of VNs, whose morphology and drainage density are “entirely consistent with rainfall and surface runoff”; (3) degraded crater morphometry is due to “modification [that] occurred by creep induced by rainsplash combined with surface runoff and erosion”; and (4) the occurrence of conditions producing “... landscapes consistent with ... possibly even oceans ....”

Our goal is to reconcile the geologic evidence for a “warm and wet” climate with 3-D GCM simulations: we assume that a LN-EH climate supporting rainfall and runoff was plausible, based on the overwhelming geologic evidence, and force above-freezing surface temperature conditions in the 3-D Laboratoire de

Météorologie Dynamique (LMD) GCM for early Mars. We first analyze model-predicted temperature and distributions of ice, rainfall, and snowfall. We then compare these results with the distribution of the VNs and lakes to provide useful insight into the possible formation conditions and driving mechanisms of these fluvial and lacustrine features. We aim to answer the following question: Can the predicted rainfall and rainfall-related erosion in a MAT  $\sim 275$  K “warm and wet” climate plausibly explain the formation of features that have previously been identified as evidence for rainfall-related processes (Ramirez & Craddock, 2018)?

## 2. Methods

We employ the 3-D LMD GCM for early Mars (Forget et al., 2013; Wordsworth et al., 2013) to simulate a “warm and wet” climate. We consider a globally averaged 1 bar CO<sub>2</sub> atmosphere (Jakosky et al., 2017), 25° and 45° obliquity (Laskar et al., 2004), a circular orbit, and 75% of the present solar luminosity (Gough, 1981). Although the atmospheric pressure may have been less than 1 bar CO<sub>2</sub> in the LN-EH, we are interested in producing the warmest possible conditions in our analysis; higher atmospheric pressure provides an increased thermal blanketing effect and thus higher global MAT. For this reason, we choose the reasonable upper limit for the LN-EH atmospheric CO<sub>2</sub> inventory as determined by recent results from the Mars Atmosphere and Volatile Evolution mission (Jakosky et al., 2017). The obliquity values we use represent approximately the reasonable lower limit ( $\sim 25^\circ$ ;  $-1\sigma$  of the mean obliquity over the past 5 Gy) and most probable value ( $\sim 45^\circ$ ) for obliquity variations over the past 5 Gy, as predicted by the statistical analysis of Laskar et al. (2004). We highlight the lower limit, in addition to the most probable value, because lower obliquity focuses maximum incident solar radiation near the equator, where the majority of the VNs and lakes are observed (Hynek et al., 2010); this effect produces warmer conditions in the near-equatorial regions. Periods of higher obliquity are likely to have existed, but we do not explore that parameter space here because higher obliquity would focus incident solar radiation, and thus temperatures  $>273$  K, toward the poles, where the fluvial/lacustrine features are not observed. Additionally, eccentricity was likely to have been higher than zero, with a predicted statistical average for the past 5 Gy of 0.069 (Laskar et al., 2004). Although theoretically, periods of relatively high eccentricity could lead to increased summer season temperatures, potentially producing summer season conditions more suitable to rainfall in the highlands, analyses of LN-EH peak and seasonal temperature distributions (Palumbo et al., 2018) suggest that changing the eccentricity within the probable LN-EH range would not lead to significant changes in the rainfall, snowfall, or MAT distributions. Thus, assuming a circular orbit is sufficient for our analysis. Finally, assuming that the Sun is a main sequence-like star, Gough (1981) estimated that solar luminosity in the LN-EH would have been approximately 75% the present value, and we adopt this value here.

Previous work has shown that these ambient conditions will naturally produce a “cold and icy” LN-EH climate (Forget et al., 2013; Wordsworth et al., 2013). A plausible combination of greenhouse gases that can produce continuous and long-lived MAT  $\geq 273$  K has not yet been identified (Forget et al., 2013). Thus, we focus on the lowest temperature end of a “warm and wet” climate (global MAT  $\sim 275$  K,  $\sim 2$  K above the melting point of water) because the least amount of required greenhouse warming is considered to be the most plausible. We note that 273 K is  $\sim 50$  K above the ambient “cold and icy” climate. Because a plausible combination of greenhouse gases that can produce this continuous and long-lived “warm and wet” climate has not yet been identified, we artificially warm the planet by introducing a gray gas into the model atmosphere. A gray gas uniformly absorbs across the infrared spectrum at all wavelengths with a defined absorption coefficient,  $\kappa$ . We choose  $\kappa = 7.5 \times 10^{-5} \frac{\text{m}^2}{\text{kg}}$  for the 25° obliquity simulation and  $\kappa = 9.5 \times 10^{-5} \frac{\text{m}^2}{\text{kg}}$  for 45° obliquity, which produces the desired climate, with MAT  $\sim 273$  K in the near-equatorial regions where VNs/lakes are abundant and global MAT is  $\sim 275$  K.

We run the GCM at a spatial resolution of  $64 \times 48 \times 25$  (longitude  $\times$  latitude  $\times$  altitude) and collect hourly data. These spatial and temporal resolutions are sufficient to capture necessary regional and seasonal variations. We have ensured that the model has reached equilibrium before analyzing the data; the results shown here are not influenced by the initial surface water/ice distribution. Further, simulations shown here include a global water inventory of  $\sim 5$  m global equivalent layer (GEL), in line with lower limit estimates for the amount of water required to carve the VNs (minimum 3 m GEL; Rosenberg & Head, 2015). We have confirmed that the model has sufficient volumes of water to accurately predict rainfall and snowfall patterns because we have produced similar simulations with 34 m GEL water (likely upper limit for the Noachian; Carr & Head, 2015)

and rainfall is concentrated in the same regions. The physics, chemistry, and physical parameterizations for this version of the GCM implemented here is described in detail by Wordsworth et al. (2015) and includes a full water cycle, advanced ice equilibration methodology for accuracy and time efficiency, cloud nucleation dynamics and microphysics, tracers for both CO<sub>2</sub> and H<sub>2</sub>O molecules, and Mars Orbiter Laser Altimeter topography. We use present-day topography, assuming that the major impact basins and volcanic rises had formed by the LN-EH (Fassett & Head, 2011).

To better understand the climatic characteristics of a “warm and wet” climate, we analyze the simulated climate on the basis of the factors deemed necessary to explain the formation of the VNs and lakes, temperatures  $\geq 273$  K and rainfall. We determine regions of the planet that experience temperatures  $\geq 273$  K and rainfall and how these patterns vary seasonally. Then we perform a spatial correlation between areas with temperatures  $\geq 273$  K and the distributions of the VNs (from Hynes et al., 2010) and lakes (from Fassett & Head, 2008b; Goudge et al., 2015) and areas with rainfall and the distributions of the VNs/lakes. Specifically, we determine whether the VNs and lakes are within regions characterized by rainfall and temperatures  $\geq 273$  K, based on the assumption that if liquid water were to run off on the surface and incise a VN, the head (source region) of the channel would have to be at a location where rainfall occurred. We are also interested in whether or not ice is stable anywhere on the planet and if, and where, snowfall occurs, which are important factors for characterizing the global hydrological system and water sinks on the surface. The aim is to determine whether the fluvial and lacustrine features could have formed in a “warm and wet” climate or whether they are inconsistent with this climate scenario. In the latter case, we consider that the formation of these features may have required even warmer and wetter conditions by reflecting on the results of previous work by Wordsworth et al. (2015) which simulated a rainfall-dominated climate with Earth-like MAT (~283 K) or that they formed through punctuated ice melting and runoff in a predominantly “cold and icy” climate (Head et al., 2017). We then use our results to address the four main predictions of Craddock and Howard (2002) and Ramirez and Craddock (2018).

### 3. Results and Discussion

The current Mars atmosphere is so tenuous (~7 mbar) that it is not thermally coupled to the surface, and surface temperatures vary primarily as a function of latitude, with warmer temperatures focused near the equator and colder temperatures focused near the poles. However, for atmospheric pressures above a few tens of millibars, the atmosphere becomes thermally coupled to the surface and an adiabatic cooling effect becomes the prominent mechanism for heat transport through the atmosphere. Because of the large topographic variations across the surface of Mars and relatively high atmospheric density, the adiabatic cooling effect causes temperature to be dominantly altitude-dependent (Forget et al., 2013; Wordsworth et al., 2015, 2013), instead of dominantly latitude-dependent. Thus, higher altitude surfaces act as cold traps for water, and ice becomes stable at high altitudes year-round. In the typical “cold and icy” scenario, ice is cold-trapped in the southern highlands because of this effect. In the “warm and wet” global MAT ~275 K simulations analyzed here (Figure 1), for the case of 25° obliquity, the highest altitude region, the Tharsis rise, and the south polar region are consistently below 273 K year-round and some water is cold-trapped in these regions as ice (Figure 1b). In the 45° obliquity simulation, relatively more solar insolation reaches the south polar region and the only part of the planet that is consistently below 273 K is the highest altitude region, the Tharsis rise, and some water is cold-trapped there (Figure 1b). In addition to this cold-trapping effect, volumes of annually accumulated snow outweigh volumes of melted snow in many areas of the highlands, causing areas in the highlands that are not permanent cold traps to contain some surface snow/ice throughout the entire year (Figure 1c). At locations where ice is present year-round, the surface is never exposed to the atmosphere, implying that overland flow and surface erosion at those locations is not possible. On the other hand, at locations where the minimum amount of ice present over the course of one year is zero, any snow/ice that accumulated at that location is melted during periods of relatively warm conditions, such as the summer season. At these locations, the surface is exposed to the atmosphere for at least part of the year, allowing for surface erosion by runoff of meltwater or rainfall. To determine the locations of regions that contain surface snow/ice throughout the entire year, we calculate the minimum volume of surface snow/ice at each latitude/longitude GCM grid cell. The distribution of regions that contain snow/ice throughout the year is shown in Figure 1c.

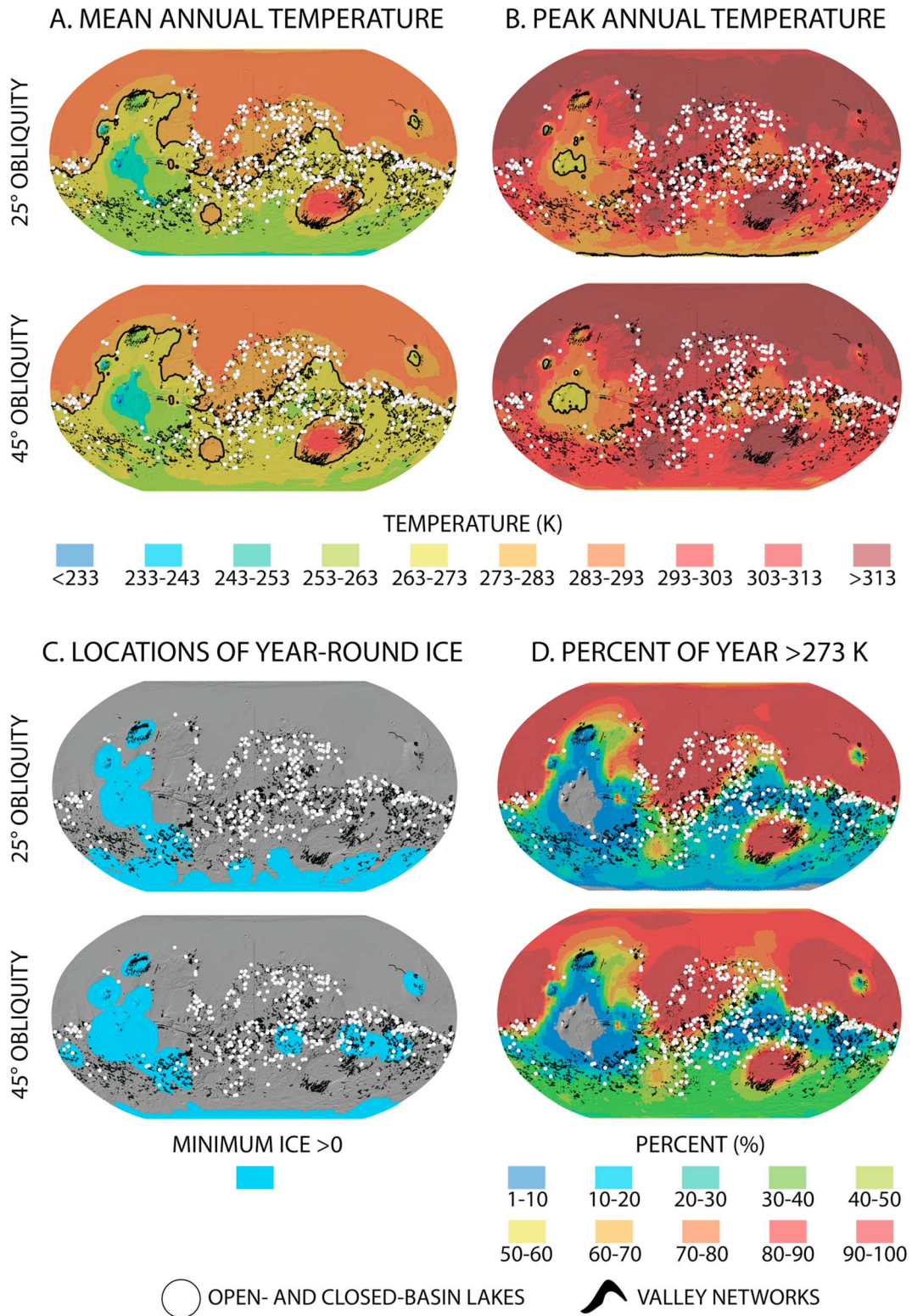


**Figure 1.** Results from simulations. (a) Mean annual temperature and (b) peak annual temperature maps. (c) Locations where ice is present year-round. (d) Percent of the year above freezing. This is calculated by number of data points per year above freezing which is a reasonable approximation because we utilize hourly data. Results are for 25° (top) and 45° (bottom) obliquity. The black line in (a) and (b) is the 273 K isotherm. Valley networks are black lines (from Hynek et al., 2010), and lakes (from Fassett & Head, 2008b; Goudge et al., 2015) are filled white circles.

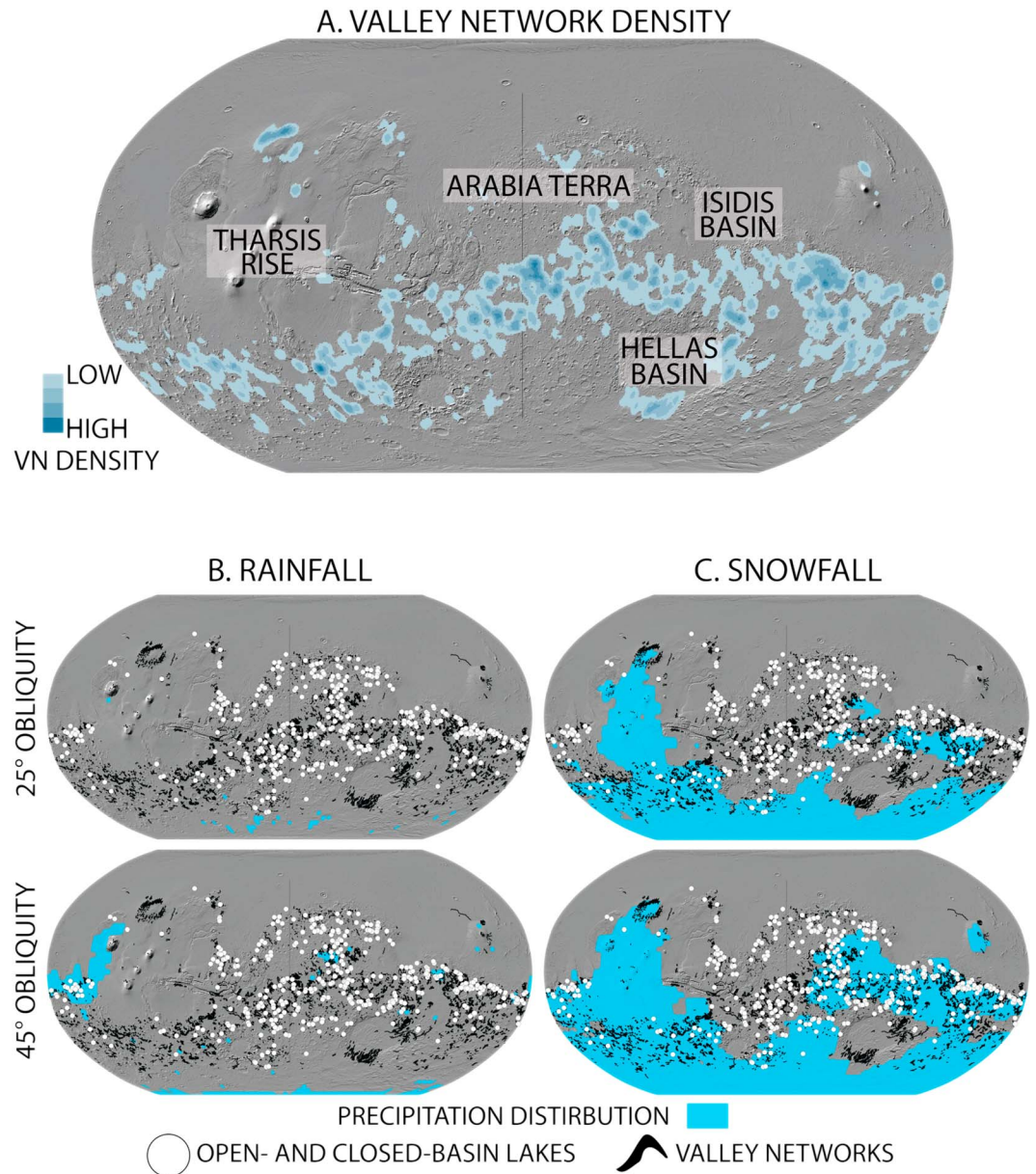


**Figure 2.** (a) VN density map (data from Hynek et al., 2010). Major topographic features that are referred to in the text are labeled. Lighter shades of blue represent lower density; darker shades represent higher density. (b) Distribution of locations where rainfall occurs and (c) distribution of locations where snowfall occurs for both simulations done here, 25° obliquity (top) and 45° obliquity (bottom). In (b) and (c), VNs and lakes are shown as black lines and filled white circles, respectively. VN = valley network.

### 3.1. Case 1: 25° Obliquity

The global MAT is above the melting point of water (~275 K), but the altitude dependence of temperature means that vast portions of the highlands have local MAT < 273 K (Figure 1a). In Figure 1a, regions with MAT > 273 K are indicated by the black line, the 273 K contour. With respect to the 273 K contour, regions shaded in warmer colors have MAT > 273 K (reds and oranges) and regions shaded in cooler colors have MAT < 273 K (yellows, greens, and blues). Areas with abundant VNs and lakes and MAT ≥ 273 K (Figures 1a and 2a) include Arabia Terra, near the south-eastern rim of Hellas basin, near the rim of Isidis basin, and regions in close proximity to the dichotomy boundary; in general, however, regions with high VN density are not located in regions with MAT ≥ 273 K (Figure 1a). In total, ~33% of the VNs mapped by Hynek et al.

(2010) and ~54% of the lakes mapped by Goudge et al. (2015) and Fassett and Head (2008) are located within regions with  $\text{MAT} \geq 273$  K. It is important to note, however, that the Hynek et al. (2010) database includes some mapped fluvial features that are not typical VNs. Specifically, fretted channels in the Arabia Terra region and outflow channels and associated networks in the Hellas basin region are included in these maps. Because the majority of the VNs that are consistent with locations where local  $\text{MAT} \geq 273$  K are within the Arabia Terra and SE Hellas rim regions (Figure 1a), we note that this correlation may be artificially increased by these non-VN fluvial features.

Seasonal variations increase temperatures to  $>273$  K in the warmest parts of the summer season, producing peak annual temperatures (PAT)  $>273$  K for most of the planet (Figure 1b). These temperatures are relatively short lived in the highlands, however, persisting for only the warmest parts of the summer season (Figure 1d). For a scenario with higher eccentricity and therefore a higher magnitude of seasonal temperature variations, the PAT would be higher, but the duration of temperature  $\geq 273$  K at any location would be generally similar (Palumbo et al., 2018) within the plausible range of Noachian eccentricity values (Laskar et al., 2004). As a result of the fact that the majority of the year is characterized by temperatures  $<273$  K in the highlands, most precipitation occurs as snowfall instead of rainfall (Figures 2b and 2c; snowfall occurs on ~31% of the planet, while rainfall occurs on ~0.8% of the planet). The distribution of locations that experience rainfall is very limited, with only a few locations where rainfall occurs; all of the locations in which rainfall occurs are in the highlands (see rainfall distributions in Figure 2b) due to the adiabatic cooling effect which causes water to be deposited in the highlands, not the lowlands. None of the regions in which rainfall occurs are correlated with areas with  $\text{MAT} \geq 273$  K, implying that even when rainfall does occur, the location where rainfall occurs is likely to return to temperatures  $<273$  K rapidly (Figure 1d) and the surrounding regions are likely to be characterized by temperatures  $<273$  K, causing the liquid water to rapidly freeze. In other words, the very small amount of rainfall that does occur in the  $\text{MAT} \sim 275$  K model is associated with peak summertime conditions in the highlands. Due to the general atmospheric circulation in the modeled climate and the fact that our simulations do not force the long-lived presence of a standing body of water in the lowlands, precipitation does not occur within the northern lowlands, where temperatures  $\geq 273$  K are more widespread and persist for longer durations. The lowlands are warmer than the highlands because temperature is dominantly dependent on altitude. However, the adiabatic cooling effect causes water to be deposited as ice in the highlands; the major sink for water is the highlands. Summertime melting will allow the ice to melt and run off down-slope, temporarily ponding in the lowlands, but the adiabatic cooling effect will cause it to be naturally redeposited as snow in the highlands. We note that a larger global water inventory may permit thicker cold-season ice sheets in the highlands and, in turn, a larger volume of summertime meltwater which could seasonally pond in the lowlands before it is transported back to the highlands in colder seasons. This is in contrast to expected circulation patterns in the presence of a northern hemispheric ocean—the ocean is a major water source and will initiate hydrological cycling in the lowlands, in addition to the hydrological cycling in the highlands, as the water is slowly transported to the highlands, where it will be redeposited as surface ice (e.g., Kreslavsky & Head, 2002; Turbet et al., 2017). Upon redeposition of all water from the ocean to the highlands, the precipitation patterns are expected to be similar to the results shown here.

Additionally, locations that experience rainfall are not correlated with the distribution of VNs and lakes (Figure 2b), mainly because the regions with rainfall cover such a small surface area ( $<1\%$  of the planet). Thus, the distribution of VNs and lakes is inconsistent with formation through rainfall-related erosion in this simulated climate that is characterized by globally averaged surface temperatures that are above freezing.

Instead of rainfall, widespread snowfall occurs across most of the highlands (Figure 2c). In low latitudes and near equatorial regions, the snowfall distribution coincides with the location of many VNs and lakes (Figure 2c). Specifically, ~33% of the VNs mapped by Hynek et al. (2010) and ~16% of the lakes mapped by Fassett and Head (2008b) and Goudge et al. (2015) are located in regions where snowfall occurs at some point in the year. Generally, snowfall is regionally widespread in the highlands, in the same areas as the lake distribution and regions of both high density and low density of VNs (Figure 2a).

### 3.2. Case 2: 45° Obliquity

The results of the higher obliquity simulation are broadly similar to those of the 25° obliquity simulation (Figure 1).  $\text{MAT}$  is  $\geq 273$  K for the vast majority of the lowlands, but  $\text{MAT}$  is generally  $<273$  K in the highlands due to the altitude dependence of temperature and the adiabatic cooling effect (Figure 1a). In the

summertime, peak surface temperatures are  $\geq 273$  K across most of the planet (Figure 1b), permitting minor amounts of localized rainfall (Figure 2b), but precipitation is again dominated by snowfall. Specifically,  $\sim 4\%$  of the VNs mapped by Hynek et al. (2010) and  $\sim 8\%$  of the lakes mapped by Fassett and Head (2008) and Goudge et al. (2015) are located in regions where rainfall occurs at some point in the year. On the other hand,  $\sim 68\%$  of the VNs mapped by Hynek et al. (2010) and  $\sim 55\%$  of the lakes mapped by Fassett and Head (2008) and Goudge et al. (2015) are located in regions where snowfall occurs at some point in the year.

The rainfall that does occur is predominantly focused near the south pole and west of Tharsis (Figure 2b; rainfall occurs on  $\sim 7\%$  of the planet and snowfall occurs on  $\sim 42\%$  of the planet) because precipitation is most abundant in these two regions and temperatures exceed 273 K in these regions in the summer (Figure 1b), permitting seasonal rainfall instead of snowfall. Rainfall is observed to the west, but not east, of the Tharsis rise because there is a rain shadow effect induced by the relatively high slopes and increase in elevation associated with Tharsis; warm, moist air approaches the rise in westerly winds and cools as it rises which causes the moisture to condense into rainfall, leaving dry air to advance down the eastern slope of Tharsis. There is more rainfall in the  $45^\circ$  obliquity simulation than the  $25^\circ$  obliquity simulation because temperatures in the  $25^\circ$  obliquity simulation are consistently below 273 K in the south polar region, one of only two locations where rainfall is observed in this simulation. In a manner similar to the  $25^\circ$  obliquity simulation, most of the rainfall does not occur within regions of  $\text{MAT} \geq 273$  K, implying that the rainwater would rapidly freeze. In the  $45^\circ$  obliquity simulation (Figure 2c), snowfall is distributed across more of the highlands than the lower obliquity simulation ( $25^\circ$ ); a larger percentage of the equatorial region experiences snowfall.

Approximately 24% of the VNs mapped by Hynek et al. (2010) and  $\sim 43\%$  of the lakes mapped by Goudge et al. (2015) and Fassett and Head (2008) are located within regions with  $\text{MAT} \geq 273$  K. The VNs and lakes that correspond to regions with  $\text{MAT} \geq 273$  K are mostly distributed within Arabia Terra and the SE rim of the Hellas basin, and a smaller percentage of the VNs and lakes that correspond to regions with  $\text{MAT} \geq 273$  K are distributed along the dichotomy boundary (Figure 1a). Because a majority of the mapped VNs in the Arabia Terra and Hellas basin regions mapped by Hynek et al. (2010) are not VNs but are instead fretted channels and outflow channels, almost no LN-EH VNs are distributed in regions with  $\text{MAT} \geq 273$  K.

### 3.3. Summary

We have analyzed two artificially simulated “warm and wet” climates, with  $25^\circ$  and  $45^\circ$  obliquity. We have compared the distribution of temperatures  $\geq 273$  K, rainfall, and snowfall with the observed distribution of VNs and lakes. We now use our results to test the predictions and points outlined in Craddock and Howard (2002) and Ramirez and Craddock (2018).

1. *Rainfall occurs “at least seasonally, if not persistently.”* Rainfall did indeed occur in both of our simulations with global  $\text{MAT} \sim 275$  K but only seasonally (during peak summer temperatures, Figure 2b) in very restricted regions, mostly located at southern high latitudes and altitudes and west of the Tharsis rise. We utilized the hourly GCM data to constrain the annual duration of rainfall and percent of the year in which rainfall occurs at each latitude/longitude GCM grid point. In the  $45^\circ$  obliquity simulation, rainfall occurs on  $\sim 7\%$  of the planet and persists for a maximum of  $\sim 5\%$  of the year. In most locations, however, rainfall persists for less than  $\sim 2$  days. In the  $25^\circ$  obliquity simulation, rainfall occurs on  $\sim 0.8\%$  of the planet and persists for a maximum of  $\sim 1.5\%$  of the year.
2. *Rainfall patterns and locations are coincident with the occurrence and density of VNs, whose morphology and drainage density are “entirely consistent with rainfall and surface runoff.”* Based on the temperature and precipitation distributions, the formation of the VNs and lakes appears broadly inconsistent with formation through rainfall-related erosion in the modeled  $\text{MAT} \sim 275$  K “warm and wet” climates.
3. *Degraded crater morphometry is due to “modification [that] occurred by creep induced by rainsplash combined with surface runoff and erosion.”* The climate simulated in this study is inconsistent with rainfall as the driving mechanism for crater degradation and surface aqueous alteration due to the fact that the dominant form of precipitation is snowfall and rainfall is not widespread or voluminous in the highlands. Future studies should test other mechanisms to explain the degraded crater morphometry that do not require rainsplash-related erosion.
4. *“... landscapes consistent with ... possibly even oceans ...”* In our simulations, we found that water in the lowlands would be rapidly transported to the highlands and be reprecipitated as snow. During the summer, some of the surface snow/ice will melt and run off on the surface but will be transported back to the

highlands as snow/ice in the colder seasons. In some locations, such as the Tharsis rise (25° and 45° obliquity) and the south polar region (25° obliquity), water is trapped as ice year-round. This description of the global hydrological cycle is not consistent with a stable or long-lived overland flow-fed ocean in the lowlands.

Despite the warm 275 K MAT climate, (1) the fluvial and lacustrine features and the observed crater degradation are unable to be explained through rainfall in this climate scenario, (2) the lack of widespread, persistent rainfall and elevated temperatures, and the significant areas covered by long-term snow and ice cover, do not favor the formation of widely distributed aqueous alteration products, and (3) a long-lived overland flow-fed ocean in the lowlands is not predicted.

How much higher would MAT need to be to induce more widespread rainfall? Wordsworth et al. (2015) simulated a warmer climate scenario (~283 K) with a (forced) stable northern ocean and found that precipitation is dominated by rainfall, instead of snowfall. However, although there is abundant rainfall, the distribution of VNs and lakes is inconsistent with the distribution of rainfall in many regions (Wordsworth et al., 2015). Thus, increasing temperatures even further leads to more areas that experience rainfall but does not appear to offer a rainfall-related explanation for VN and lake formation. Wordsworth et al. (2015) found that snowfall in a “cold and icy” climate, and associated seasonal or punctuated melting, is better correlated with the VN distribution than rainfall in a “warm and wet” climate. Under these warmer MAT ~283 K conditions, rainfall is widespread, and it is important to note that a rainsplash-related explanation for degraded crater rims and aqueous mineral alteration at the surface in the highlands is more plausible than in the MAT ~275 K climate that we simulate in this study.

#### 4. Conclusions

Using the 3-D LMD GCM for early Mars, we have simulated a “warm and wet” climate, characterized by global MAT ~275 K and equatorial MAT ~273 K. Rainfall is limited, precipitation is dominated by snowfall, and temperatures in the highlands are <273 K for the majority of the year. Many of VNs and lakes, as well as degraded craters, occur in areas of snowfall, not rainfall, and the global distribution of water is dominated by ice in the highlands and near the Tharsis rise, not by an ocean or global liquid water that might form surface clays. The ability to form surface clays in colder conditions, possibly through seasonal snowmelt, requires a better understanding of the temperature, water volume, and duration constraints for in situ clay formation (e.g., Bishop et al., 2017).

The transition from a snowfall-dominated to a rainfall-dominated climate (Wordsworth et al., 2015) occurs at global MAT >275 K and <283 K. Even at MAT 283 K, the distribution of VNs is not well correlated with predicted rainfall patterns (Wordsworth et al., 2015). Thus, we suggest that shorter-term transient warm temperature phases in an otherwise “cold and icy” background climate (e.g., Head & Marchant, 2014; Wordsworth et al., 2015), permitting transient melting of surface snow/ice and liquid water runoff, might be more likely to explain the formation of the VNs and lakes than rainfall in a “warm and wet” climate. In other words, we suggest that the VNs and lakes, which are commonly cited as the most robust evidence for “warm and wet” Late Noachian conditions, might be better explained by a “cold and icy” climate.

#### Acknowledgments

This work was supported by NASA Headquarters under the NASA Earth and Space Science Fellowship Program for AMP, grant 90NSSC17K0487. The authors would like to thank Robin Wordsworth for his continued guidance for use of the LMD GCM and helpful input regarding the development of this manuscript and Michael Mischna and Ralf Jaumann for helpful reviews. GCM data used in this analysis are available on the Brown Planetary Geosciences Research Database: [http://www.planetary.brown.edu/html\\_pages/data.htm](http://www.planetary.brown.edu/html_pages/data.htm).

#### References

- Achille, G. D., & Hynek, B. M. (2010). Ancient ocean on Mars supported by global distribution of deltas and valleys. *Nature Geoscience*, 3(7), 459–463. <https://doi.org/10.1038/ngeo891>
- Bibring, J.-P., Langevin, Y., Mustard, J., Poulet, F., Arvidson, R., Gendrin, A., & the OMEGA team (2006). Global mineralogical and aqueous Mars history derived from OMEGA/Mars Express data. *Science*, 312(5772), 400–404. <https://doi.org/10.1126/science.1122659>
- Bishop, J., Baker, L., Fairen, A., Gross, C., Velbel, M., Rampe, E., & Michalski, J. (2017). Unraveling the diversity of early aqueous environments and climate on Mars through the phyllosilicate record. 48<sup>th</sup> LPSC, Abstract 1804.
- Cabrol, N. A., & Grin, E. A. (1999). Distribution, classification, and ages of Martian impact crater lakes. *Icarus*, 142(1), 160–172. <https://doi.org/10.1006/icar.1999.6191>
- Carr, M., & Head, J. (2015). Martian surface/near-surface water inventory: Sources, sinks, and changes with time. *Geophysical Research Letters*, 42, 726–732. <https://doi.org/10.1002/2014GL062464>
- Carter, J., Loizeau, D., Mangold, N., Poulet, F., & Bibring, J.-P. (2015). Widespread surface weathering on early Mars: A case for a warmer and wetter climate. *Icarus*, 248, 373–382. <https://doi.org/10.1016/j.icarus.2014.11.011>
- Clifford, S. M. (1993). A model for the hydrologic and climatic behavior of water on Mars. *Journal of Geophysical Research*, 98(E6), 10,973–11,016. <https://doi.org/10.1029/93JE00225>
- Craddock, R. A., & Howard, A. D. (2002). The case for rainfall on a warm, wet early Mars. *Journal of Geophysical Research*, 107(E11), 5111. <https://doi.org/10.1029/2001JE001505>

- Fassett, C. I., & Head, J. W. (2008a). The timing of Martian valley network activity: Constraints from buffered crater counting. *Icarus*, *195*(1), 61–89. <https://doi.org/10.1016/j.icarus.2007.12.009>
- Fassett, C. I., & Head, J. W. (2008b). Valley network-fed, open-basin lakes on Mars: Distribution and implications for Noachian surface and subsurface hydrology. *Icarus*, *198*(1), 37–56. <https://doi.org/10.1016/j.icarus.2008.06.016>
- Fassett, C. I., & Head, J. W. (2011). Sequence and timing of conditions on early Mars. *Icarus*, *211*(2), 1204–1214. <https://doi.org/10.1016/j.icarus.2010.11.014>
- Forget, F., Wordsworth, R., Millour, E., Madeleine, J.-B., Kerber, L., Leconte, J., et al. (2013). 3D modelling of the early Martian climate under a denser CO<sub>2</sub> atmosphere: Temperatures and CO<sub>2</sub> ice clouds. *Icarus*, *222*(1), 81–99. <https://doi.org/10.1016/j.icarus.2012.10.019>
- Goudge, T. A., Aureli, K. L., Head, J. W., Fassett, C. I., & Mustard, J. F. (2015). Classification and analysis of candidate impact crater-hosted closed-basin lakes on Mars. *Icarus*, *260*, 346–367. <https://doi.org/10.1016/j.icarus.2015.07.026>
- Gough, D. O. (1981). Solar interior structure and luminosity variations. *Solar Physics*, *74*(1), 21–34. <https://doi.org/10.1007/BF00151270>
- Halevy, I., & Head, J. W. (2014). Episodic warming of early Mars by punctuated volcanism. *Nature Geoscience*, *7*(12), 865–868. <https://doi.org/10.1038/ngeo2293>
- Head, J., & Marchant, D. (2014). The climate history of early Mars: Insights from the Antarctic McMurdo dry valleys hydrologic system. *Antarctic Science*, *26*(06), 774–800. <https://doi.org/10.1017/S0954102014000686>
- Head, J., Wordsworth, R., Forget, F., & Turbet, M. (2017). Deciphering the Noachian geological and climate history of Mars: Part 2—A Noachian stratigraphic view of major geologic processes and their climatic consequences, in: 4th International Conference on Early Mars. Presented at the 4th International Conference on Early Mars, Flagstaff, AZ.
- Hynek, B. M., Beach, M., & Hoke, M. R. T. (2010). Updated global map of Martian valley networks and implications for climate and hydrologic processes. *Journal of Geophysical Research*, *115*, E09008. <https://doi.org/10.1029/2009JE003548>
- Jakosky, B. M., Slipski, M., Benna, M., Mahaffy, P., Elrod, M., Yelle, R., et al. (2017). Mars' atmospheric history derived from upper-atmosphere measurements of <sup>38</sup>Ar, <sup>36</sup>Ar. *Science*, *355*(6332), 1408–1410. <https://doi.org/10.1126/science.aai7721>
- Johnson, S. S., Mischna, M., Grove, T., & Zuber, M. (2008). Sulfur-induced greenhouse warming on early Mars. *Journal of Geophysical Research*, *113*, E08005. <https://doi.org/10.1029/2007JE002962>
- Jones, K. L. (1974). Evidence for an episode of crater obliteration intermediate in Martian history. *Journal of Geophysical Research*, *79*(26), 3917–3931. <https://doi.org/10.1029/JB079i026p03917>
- Kreslavsky, M., & Head, J. (2002). Fate of outflow channel effluents in the northern lowlands of Mars: The Vastitas Borealis formation as a sublimation residue from frozen bodies of water. *Journal of Geophysical Research*, *107*(E12), 5121. <https://doi.org/10.1029/2001JE001831>
- Laskar, J., Correia, A. C. M., Gastineau, M., Joutel, F., Levrard, B., & Robutel, P. (2004). Long term evolution and chaotic diffusion of the insolation quantities of Mars. *Icarus*, *170*(2), 343–364. <https://doi.org/10.1016/j.icarus.2004.04.005>
- Luo, W., Cang, X., & Howard, A. D. (2017). New Martian valley network volume estimate consistent with ancient ocean and warm and wet climate. *Nature Communications*, *8*, 15766. <https://doi.org/10.1038/ncomms15766>
- Mischna, M., Baker, V., Milliken, R., Richardson, M., & Lee, C. (2013). Effects of obliquity and water vapor/trace gas greenhouses in the early Martian climate. *Journal of Geophysical Research: Planets*, *118*, 560–576. <https://doi.org/10.1002/jgre.20054>
- Palumbo, A., Head, J., & Wordsworth, R. (2018). Late Noachian icy highlands climate model: Exploring the possibility of transient melting and fluvial/lacustrine activity through peak annual and seasonal temperatures. *Icarus*, *300*, 261–286. <https://doi.org/10.1016/j.icarus.2017.09.007>
- Parker, T., Gorsline, D., Saunders, R., Pieri, D., & Schneeberger, D. (1993). Coastal geomorphology of the Martian northern plains. *Journal of Geophysical Research*, *98*(E6), 11,061–11,078. <https://doi.org/10.1029/93JE00618>
- Postawko, S. E., & Kuhn, W. R. (1986). Effect of the greenhouse gases (CO<sub>2</sub>, H<sub>2</sub>O, SO<sub>2</sub>) on Martian paleoclimate. *Journal of Geophysical Research*, *91*(B4), 431–438. <https://doi.org/10.1029/JB091iB04p0431>
- Ramirez, R., & Craddock, R. (2018). The geological and climatological case for a warmer and wetter early Mars. *Nature Geoscience*, *11*(4), 230–237. <https://doi.org/10.1038/s41561-018-0093-9>
- Ramirez, R. M. (2017). A warmer and wetter solution for early Mars and the challenges with transient warming. *Icarus*, *297*, 71–82. <https://doi.org/10.1016/j.icarus.2017.06.025>
- Rosenberg, E., & Head, J. (2015). Late Noachian fluvial erosion on Mars: Cumulative water volumes required to carve the valley networks and grain size of bed-sediment. *Planetary and Space Science*, *117*, 429–435. <https://doi.org/10.1016/j.pss.2015.08.015>
- Turbet, M., Forget, F., Head, J., & Wordsworth, R. (2017). 3D modelling of the climatic impact of outflow channel formation events on early Mars. *Icarus*, *228*, 10–36.
- Wordsworth, R., Forget, F., Millour, E., Head, J. W., Madeleine, J.-B., & Charnay, B. (2013). Global modelling of the early Martian climate under a denser CO<sub>2</sub> atmosphere: Water cycle and ice evolution. *Icarus*, *222*(1), 1–19. <https://doi.org/10.1016/j.icarus.2012.09.036>
- Wordsworth, R., Kerber, L., Pierrehumbert, R., Forget, F., & Head, J. (2015). Comparison of “warm and wet” and “cold and icy” scenarios for early Mars in a 3-D climate model. *Journal of Geophysical Research: Planets*, *120*, 1201–1219. <https://doi.org/10.1002/2015JE004787>